

1 **Discovery of a new genus of anaerobic ammonium oxidizing bacteria**
2 **with a mechanism for oxygen tolerance**

3
4 Yuchun Yang^{1, #}, Zhongyi Lu^{2, 3, #}, Mohammad Azari⁴, Boran Kartal⁶, Huan Du², Mingwei
5 Cai², Craig W. Herbold⁸, Xinghua Ding⁷, Martin Denecke⁵, Xiaoyan Li⁹, Meng Li², and Ji-
6 Dong Gu^{10, 11, 12, *}

7
8 ¹ State Key Laboratory of Biocontrol, School of Ecology, Sun Yat-sen University, Guangzhou
9 510275, People's Republic of China

10 ² Shenzhen Key Laboratory of Marine Microbiome Engineering, Institute for Advanced Study,
11 Shenzhen University, Shenzhen 518060, People's Republic of China

12 ³ Key Laboratory of Optoelectronic Devices and Systems of Ministry of Education and
13 Guangdong Province, College of Optoelectronic Engineering, Shenzhen University, Shenzhen
14 518060, People's Republic of China

15 ⁴ Department of Aquatic Environmental Engineering, Institute for Water and River Basin
16 Management, Karlsruhe Institute of Technology (KIT), Gotthard-Franz-Str. 3, Karlsruhe
17 76131, Germany

18 ⁵ Department of Urban Water- and Waste Management, University of Duisburg-Essen,
19 Universitätsstraße 15, 45141 Essen, Germany

20 ⁶ Microbial Physiology Group, Max Planck Institute for Marine Microbiology, Celsiusstraße 1,
21 28359 Bremen, Germany

22 ⁷ Laboratory of Environmental Microbiology and Toxicology, School of Biological Sciences,
23 The University of Hong Kong, Pokfulam Road, Hong Kong SAR, Hong Kong, People's
24 Republic of China

25 ⁸ University of Vienna, Centre for Microbiology and Environmental Systems Science, Division
26 of Microbial Ecology, Althanstrasse 14, 1090 Vienna, Austria

27 ⁹ Department of Civil Engineering, The University of Hong Kong, Pokfulam Road, Hong Kong
28 SAR, Hong Kong, People's Republic of China

29 ¹⁰ Environmental Science and Engineering Research Group, Guangdong Technion - Israel
30 Institute of Technology, 241 Daxue Road, Shantou, Guangdong 515063, People's Republic of
31 China

32 ¹¹ Southern Laboratory of Ocean Science and Engineering (Guangdong, Zhuhai), Zhuhai,
33 Guangdong 519082, People's Republic of China

34 ¹²Guangdong Provincial Key Laboratory of Materials and Technologies for Energy Conversion,
35 Guangdong Technion – Israel Institute of Technology, 241 Daxue Road, Shantou, Guangdong
36 515063, People’s Republic of China

37

38 # Authors contributed equally to this work

39

40 *Corresponding author

41 Ji-Dong Gu, e-mail: jidong.gu@gtiit.edu.cn

42

43 **Abstract**

44 In the past 20 years, there has been a major stride in understanding the core mechanism of
45 anaerobic ammonium-oxidizing (anammox) bacteria, but there are still several discussion
46 points on their survival strategies. Here, we discovered a new genus of anammox bacteria in a
47 full-scale wastewater-treating biofilm system, tentatively named “*Candidatus* Loosdrehtia
48 aerotolerans”. Next to genes of all core anammox metabolisms, it encoded and transcribed
49 genes involved in the dissimilatory nitrate reduction to ammonium (DNRA), which coupled to
50 oxidation of small organic acids, could be used to replenish ammonium and sustain their
51 metabolism. Surprisingly, it uniquely harbored a new ferredoxin-dependent nitrate reductase,
52 which has not yet been found in any other anammox genome and might confer a selective
53 advantage to it in nitrate assimilation. Similar to many other microorganisms, superoxide
54 dismutase and catalase related to oxidative stress resistance were encoded and transcribed by
55 “*Ca. Loosdrehtia aerotolerans*”. Interestingly, bilirubin oxidase (BOD), likely involved in
56 oxygen resistance of anammox bacteria under fluctuating oxygen concentrations, was
57 identified in “*Ca. Loosdrehtia aerotolerans*” and four *Ca. Brocadia* genomes, and its activity
58 was demonstrated using purified heterologously expressed proteins. A following survey of
59 oxygen-active proteins in anammox bacteria revealed the presence of other previously
60 undetected oxygen defense systems. The novel *cbb3*-type cytochrome c oxidase and
61 bifunctional catalase-peroxidase may confer a selective advantage to *Ca. Kuenenia* and *Ca.*
62 *Scalindua* that face frequent changes in oxygen concentrations. The discovery of this new
63 genus significantly broadens our understanding of the ecophysiology of anammox bacteria.
64 Furthermore, the diverse oxygen tolerance strategies employed by distinct anammox bacteria
65 advance our understanding of their niche adaptability and provide valuable insight for the
66 operation of anammox-based wastewater treatment systems.

67

68 **Keywords:**

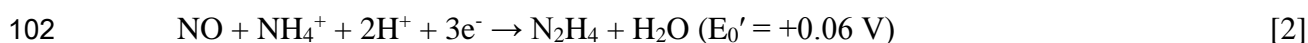
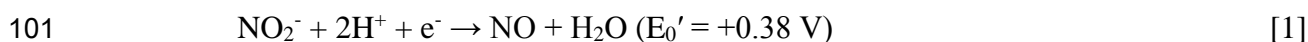
69 Anammox, New genus, Biofilm, Oxygen tolerance, Nitrate reduction

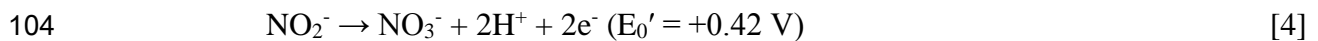
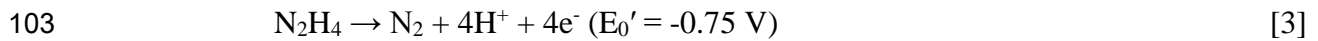
70

71 1. Introduction

72 The discovery of anaerobic ammonium oxidation (anammox) completely changed our
73 understanding of the nitrogen cycle (Kuypers et al. 2018, Mulder et al. 1995). Anammox
74 bacteria are affiliated with a monophyletic group in the phylum *Planctomycetes* (Strous et al.
75 1999), and have been detected in many natural and engineered ecosystems, where they
76 facilitate the release of fixed nitrogen into the atmosphere. After the initial discovery of the
77 anammox process, five candidate genera of anammox bacteria, including *Ca. Scalindua*
78 (Kuypers et al. 2003), *Ca. Kuenenia* (Schmid et al. 2000, Schmid et al. 2003), *Ca. Brocadia*
79 (Strous et al. 1999), *Ca. Anammoxoglobus* (Kartal et al. 2007b), and *Ca. Jettenia* (Quan et al.
80 2008), were consecutively identified.

81 Environmental metagenomics combined with continuous cultivation approaches and
82 biochemical experiments resulted in the description of the core anammox metabolism, which
83 can be described in three main catabolic reactions (Hu et al. 2019, Kartal et al. 2011): reduction
84 of nitrite (NO_2^-) to nitric oxide (NO) by nitrite reductase (NIR or an unidentified enzyme,
85 equation (1)), transformation of ammonium (NH_4^+) and NO to hydrazine (N_2H_4) by hydrazine
86 synthase (HZS, equation (2)) (Kartal et al. 2011, Maalcke et al. 2014, Oshiki et al. 2016a), and
87 oxidation of N_2H_4 into dinitrogen gas (N_2) by hydrazine dehydrogenase (HDH, equation (3)).
88 The electrons released from hydrazine oxidation are used to establish a proton motive force for
89 energy conservation and produce reducing equivalents needed for cellular anabolic activity (de
90 Almeida et al. 2016, Hu et al. 2019). Whereas, hydroxylamine (NH_2OH) was found to be the
91 intermediate of anammox process in *Ca. Brocadia* that an NH_2OH -dependent metabolism was
92 proposed for some anammox bacteria (Oshiki et al. 2016a). Anammox bacteria were assumed
93 to oxidize a part of their substrate nitrite to nitrate by a nitrite oxidoreductase (NXR, equation
94 (4)) to generate electrons for the reduction of nitrite to NO (equation [1]) (Hu et al. 2019, Kartal
95 et al. 2013). Whereas HZS, HDH, and NXR are conserved throughout the known anammox
96 genera, distinct anammox bacteria encode a cytochrome *cd*₁-type NIR (NirS), a copper-
97 containing NIR (NirK), or some alternative protein for nitrite reduction such as a multiheme
98 HAO-like protein complex (Ferousi et al. 2019, Kartal and Keltjens 2016). All of these
99 catabolic reactions occur in the membrane-bound “prokaryotic organelle” called the
100 anammoxosome, which comprises 50–70% of the cell volume (de Almeida et al. 2015).





105 While there have been advances made in understanding the core metabolism of anammox
106 bacteria, there are still several discussion points on their physiological versatility and resistance
107 to environmental factors including their alternative energy sources and oxygen defense systems.
108 Anammox bacteria were assumed to have an exclusively chemolithotrophic lifestyle, acquiring
109 energy for growth solely from anaerobic NH_4^+ oxidation, but they have the genomic potential
110 of using formate, acetate, propionate, amino acid, hydrogen, and Fe^{2+} as electron donors to
111 sustain their metabolism (Kartal et al. 2013, Lawson et al. 2020). Indeed, using enrichment
112 cultures of anammox bacteria, their growth on anaerobic oxidation of short volatile fatty acids
113 was demonstrated (Güven et al. 2005, Kartal et al. 2007b, Kartal et al. 2008, Tao et al. 2019).
114 Distinct enrichments of anammox bacteria were reported to reduce NO_3^- to produce additional
115 ammonium as a substrate for their main metabolism by dissimilatory nitrate reduction to
116 ammonium (DNRA) coupled with short volatile fatty acids oxidation (Ali et al. 2020, Güven
117 et al. 2005, Kartal et al. 2007a, Winkler et al. 2012). The known anammox bacteria appear to
118 be oxygen sensitive and dissolved oxygen is an important parameter controlling anammox
119 activity in manmade ecosystems such as wastewater treatment plants (WWTPs) (Cho et al.
120 2020, Kimura et al. 2011). Nevertheless, varying levels of oxygen tolerances were observed in
121 different enrichment cultures of anammox bacteria (Oshiki et al. 2016b), but the underlying
122 mechanisms are not yet clear, and oxygen defense systems of anammox bacteria have not been
123 characterized. Altogether, these findings indicate greater ecophysiological flexibility of
124 anammox bacteria and the presence of a specific niche for each distinct anammox genera or
125 species.

126 In this study, we present the discovery of a new anammox genus in a full-scale wastewater
127 treatment biofilm system treating landfill leachate. Using its metagenome-assembled genome
128 (MAG) and metatranscriptomes, we constructed a metabolic blueprint of this new anammox
129 bacterium. In addition, a detailed analysis of the MAG revealed a bilirubin oxidase, an enzyme
130 that could be used in oxygen resistance, whose activity was validated using heterologously
131 expressed proteins. We discuss the central metabolism of this new genus and its
132 ecophysiological versatility related to its adaptation to unfavorable and fluctuating
133 environmental conditions. Furthermore, the exploration of different oxygen defense
134 mechanisms employed by distinct anammox bacteria advances our understanding of niche
135 adaption and application of anammox bacteria in wastewater treatment systems.

136 2. Materials and Methods

137 2.1. Sample collection and sequencing

138 Two separate biofilm samples were collected from the activated carbon modules of a
139 landfill leachate treatment plant called Zentraldeponie Emscherbruch (ZDE) WWTP (Table S1,
140 Figure S1) located in Herten, Germany in November 2017 and April 2018, respectively. ZDE
141 plant was primarily operated as an activated sludge system with a conventional nitrification-
142 denitrification nitrogen removal process. The plant was upgraded in 2001 by equipping
143 ultrafiltration and activated carbon modules after activated sludge systems (Figure S1). The
144 activated carbon modules were kept at a high temperature (34 °C) and nearly neutral pH (6.8)
145 (Table S1) in which granular activated carbon acted as carrier materials for the establishment
146 of anammox biofilm (Azari et al. 2017). On average 90.0% of the influent ammonium (758
147 mg/L) was removed and oxidized by the activated sludge systems; 24.8% of the inputted
148 ammonium (76.6 mg/L), 98.5% of the inputted nitrite (45.8 mg/L), and 97.4% of the inputted
149 nitrate (13.4 mg/L) were removed by the following biofilm system (Table S1). Previously,
150 frequent sampling and independent analyses confirmed the enrichment of anammox bacteria
151 in the activated carbon modules, and anammox biofilms were shaped as spherical granules with
152 red color and different sizes (1 to 13 mm) (Azari et al. 2018, Azari et al. 2017) (Figure S1).

153 Biofilm samples collected in November 2017 were used for 16S rRNA gene high
154 throughput sequencing, samples were stored at -20 °C. The specific primer pair of 515F/806R
155 with a barcode was used to amplify the V4 regions of the total DNA. Sequencing libraries were
156 generated using TruSeq[®] DNA PCR-Free Sample Preparation Kit (Illumina, USA) and index
157 codes were added. The library quality was assessed on the Qubit@ 2.0 Fluorometer (Thermo
158 Scientific) and Agilent Bioanalyzer2100 system. Libraries were sequenced on an Illumina
159 HiSeq2500 platform with an insert size of 250 bp paired-ends. Sequences analysis was carried
160 out using QIIME (Caporaso et al. 2010). Adapters, barcodes, and primers in the raw reads were
161 trimmed off, the paired-end reads were merged using FLASH V1.2.7 and reads shorter than
162 170 bp were discarded. Chimera checking was performed by USEARCH2
163 (<https://www.biorxiv.org/content/10.1101/074252v1>) using the "Gold" database as a reference.
164 All filtered sequences were clustered into one fasta file for OTU picking with $\geq 97\%$ sequence
165 identity cutoff and taxonomy assignment against SILVA 132 released reference database.

166 Two independent biofilm samples were collected from the same site in April 2018 for
167 metagenomic and metatranscriptomic sequencing, samples for DNA isolation were stored at -

168 20 °C and samples for RNA isolation were preserved on site in LifeGuard Soil Preservation
169 Solution (Qiagen, Germany). DNA and RNA extractions and the following metagenomic and
170 metatranscriptomic sequencing methods were previously described (Yang et al. 2020c). In brief,
171 total DNA and RNA were extracted, and genomic DNA was removed following RNA
172 extraction. The ribosomal RNA was depleted from the total RNA using the Ribo-Zero rRNA
173 removal kit (Illumina, Inc., San Diego, CA, USA), and the remaining mRNA was reverse-
174 transcribed. DNA and cDNA were sequenced using an Illumina HiSeq sequencer (Illumina)
175 with 150-bp paired-end reads at GENEWIZ (Suzhou, China).

176 2.2. *De novo metagenomic assembly, binning, and quality assessment*

177 Raw shotgun sequencing reads were trimmed using BBduk (BBMap v. 36.32 - Bushnell
178 B. - sourceforge.net/projects/bbmap/) with the following parameters: ktrim=r, k=21, mink=11,
179 hdist=2, minlen=149, qtrim=r, trimq=15. Trimmed metagenomic reads were assembled using
180 Spades v. 3.10.1 (Bankevich et al. 2012) with the k-mer sizes of 21, 33, 55, 77, 99, 127. All
181 resulting scaffolds larger than 2,000 bp were binned using MetaBAT v. 2.12.1 with the setting
182 ‘- minContig 2000’ (Kang et al. 2015). The best resulting bins were chosen using DASTool
183 (https://github.com/cmks/DAS_Tool). Finally, four putative anammox bacterial MAGs were
184 identified from the metagenomic dataset by GTDB-Tk v1.1.0 (Chaumeil et al. 2019) using the
185 GTDB database (<https://doi.org/10.1101/771964>), while a novel anammox bacterial MAG
186 which was named YC1 (“*Ca. Loosdrechtia aerotolerans*”), could only be assigned to family
187 *Brocadiaceae* and could not be classified as any known genera. The completeness and level of
188 contamination of YC1 were estimated using CheckM v1.0.6 (Parks et al. 2015). YC1 was
189 further iteratively assembled using a protocol as described in a previous study (Yang et al.
190 2020a). A high-quality MAG was acquired after 70 rounds of assembly (Table S2). Trimmed,
191 paired-end metagenomic reads were mapped to the metagenomic assembly and predicted open
192 reading frames (ORFs) by Prodigal v2.6.3 (Hyatt et al. 2010) using Bowtie2 v2.2.9 (Ben and
193 Steven 2012) to calculate the genome and gene abundances as RPKM (Robinson and Oshlack
194 2010). The rRNA reads were identified and removed from metatranscriptomic datasets using
195 SortMeRNA (version 2.1) (Kopylova et al. 2012) against both the SILVA 132 database and the
196 default databases. Non-rRNA metatranscriptomic reads were mapped to the predicted ORFs by
197 BWA v0.7.17 (Li and Durbin 2009) with the default settings to calculate the gene transcription
198 as RPKM.

199
$$\text{RPKM} = (\text{number of mapped reads}) / [(\text{gene length} / 1,000) * (\text{total mapped reads} / 1,000,000)]$$

200 2.3. Genome analyses

201 The genome of “*Ca. Loosdrechtia aerotolerans*” was analyzed by the MicroScope
202 platform (<http://www.genoscope.cns.fr/agc/microscope>). The genome of “*Ca. Loosdrechtia*
203 *aerotolerans*” was further annotated by GhostKOALA, which is KEGG's internal annotation
204 tool for K number assignment of KEGG GENES using SSEARCH computation (Kanehisa et
205 al. 2016). In addition, predicted ORFs were also annotated by eggNOG-mapper (Huerta-Cepas
206 et al. 2017) and Rapid Annotation using Subsystem Technology (RAST) (Overbeek et al. 2014).
207 Predicted ORFs were also searched against the NCBI non-redundant (nr) database by BLASTP
208 using an E-value $< 10^{-5}$ as the threshold with the setting ‘-max_target_seqs 3’ to acquire more
209 annotation information. The above annotation results were summarized in [Table S3](#). Potential
210 secreted proteins with the signal peptides were identified by SignalP 4.1, Signal-BLAST, and
211 PSORTb (Frank and Sippl 2008, Thomas Nordahl et al. 2011, Yu et al. 2010).

212 2.4. Phylogenetic analyses

213 All the putative anammox bacterial operational taxonomic units (OTUs) acquired from
214 the 16S rRNA gene high throughput sequencing were used for phylogenetic analysis with all
215 the 16S rRNA genes of anammox bacteria stored in the SILVA 138 SSU database. CheckM
216 v1.0.6 was used to produce an alignment of 43 concatenated markers (Parks et al. 2015) from
217 “*Ca. Loosdrechtia aerotolerans*”, previously published anammox bacterial genomes available
218 by the end of December 2019 ([Table S4](#)), and 16 other Planctomycetes genomes. The full-
219 length 16S rRNA gene in the MAG was identified by BLASTN search against the SILVA 138
220 SSU database using an E value threshold of $< 10^{-10}$. 16S rRNA genes of anammox bacteria
221 stored in the SILVA 138 SSU database were used for phylogenetic analysis with the 16S rRNA
222 gene of “*Ca. Loosdrechtia aerotolerans*”. HzsA sequences from previously published anammox
223 bacteria and “*Ca. Loosdrechtia aerotolerans*” were used for phylogenetic analysis. Sequences
224 of respiratory nitrate reductase (NarG), ferredoxin-dependent nitrate reductase (NarB),
225 periplasmic nitrate reductase (NapA), and nitrite oxidoreductase (NxrA) were downloaded
226 from NCBI and UniProtKB and clustered by usearch -cluster_fast (Edgar 2013) with an
227 identity of 85%, respectively, the cluster representatives were used for phylogenetic analysis
228 with the putative NarB from “*Ca. Loosdrechtia aerotolerans*”. Laccase and bilirubin oxidase
229 amino acid sequences downloaded from NCBI and UniProt databases were clustered by
230 usearch -cluster_fast (Edgar 2013) with an identity of 85%, and the cluster representatives were

231 used for phylogenetic analysis with the putative bilirubin oxidases from anammox bacteria. All
232 the above sequences used for phylogenetic analysis were aligned by MAFFT online service
233 (Yamada et al. 2016), and gaps in the multiple sequence alignment were removed by trimAl
234 V1.2 with the setting '-gt 0.1'. Maximum likelihood trees were built using IQ-TREE with the
235 default settings (Nguyen et al. 2015) and visualized using iTOL (Letunic and Bork 2019). The
236 models of sequence evolution HKY+F+R2, WAG+G4, LG+G4, Q.pfam+R10, VT+R10, and
237 LG+F+R6 were chosen by ModelFinder (as implemented in IQ-TREE) to build 16S rRNA
238 gene, HzsA, NxrA, nitrate reductases, BOD, and 43 concatenated markers phylogenetic trees,
239 respectively.

240 2.5. Comparative genomic analyses

241 Average amino acid identity (AAI) was calculated between the genome of “*Ca.*
242 *Loosdrechtia aerotolerans*” and 25 previously published anammox bacterial genomes (Table
243 S4) using CompareM with the default setting (<https://github.com/dparks1134/CompareM>).
244 Unique genes of “*Ca. Loosdrechtia aerotolerans*” compared to other anammox bacteria were
245 identified by a reciprocal best BLAST (Altschul et al. 1990). BLAST hits with an E-value of
246 10^{-5} , amino acid identities < 40%, and a minimum alignment length < 50% were considered as
247 unique genes.

248 The distribution of specific genes in anammox bacterial genomes was investigated.
249 Specific gene sequences identified in known anammox bacterial genomes were downloaded
250 from NCBI depending on the annotation. Furthermore, the manually annotated Swiss-Prot
251 sequences were downloaded from UniProt and merged into the above corresponding sequence
252 pools and the BLAST databases (Table S5) were built using these downloaded sequences by
253 the makeblastdb tool of NCBI. The predicted ORFs from “*Ca. Loosdrechtia aerotolerans*” and
254 25 known anammox bacterial genomes (Table S4) were searched by BLASTP against these
255 functional gene databases with E-value < 10^{-5} , amino acid identity > 40% and minimum
256 alignment length (length of aligned query sequence/length of database sequence) > 50% (Yang
257 et al. 2020a, Yang et al. 2020b). To further examine the accuracy of gene annotation based on
258 the above custom databases, the extracted gene sequences from anammox genomes were
259 BLASTP against the NCBI RefSeq protein database with E-value < 10^{-10} , and the results were
260 manually checked.

261 2.6. Global distribution

262 The 16S rRNA gene sequence of “*Ca. Loosdrechtia aerotolerans*” was submitted to
263 IMNGS (Ilias et al. 2016) with the setting “min threshold 94.5%, min size 250 bp” to
264 investigate the occurrence of the new genus in different ecosystems. All acquired sequences
265 were searched back to the 16S rRNA gene sequence of “*Ca. Loosdrechtia aerotolerans*” with
266 E-value $< 10^{-10}$ by BLASTN and only the identity larger than 94.5% (Yarza et al. 2014) was
267 considered. In the rRNA amplicon datasets, the relative abundance of the target sequences
268 larger than 0.1% was considered.

269 2.7. *Heterologous expression and purification of bilirubin oxidases*

270 The BOD sequences from “*Ca. Loosdrechtia aerotolerans*” (E3K32_04160), “*Ca.*
271 *Brocadia caroliniensis*” (OOP56653.1), and “*Ca. Brocadia* sp. AMX2” (RIK02322.1) were
272 codon optimized by GeneDesign (<http://54.235.254.95/gd/>), synthesized (BGI Genomics Co
273 Ltd., China), and cloned into the NdeI/HindIII site of pCold-TF vector with an N-terminal His₆
274 tag and a soluble trigger factor chaperone tag (Takara Bio Co Ltd., Japan). *E. coli* BL21 (Takara
275 Bio Co Ltd., Japan) was used as the host strain for the recombinant vectors. The recombinant
276 *E. coli* were inoculated into a LB medium containing 100 µg/mL ampicillin and incubated at
277 37 °C until the OD₆₀₀ reached 0.6-0.8. Isopropyl-d-1-thiogalactopyranoside and CuSO₄ were
278 added to the culture at final concentrations of 0.1 mM and 0.25 mM, respectively, and then the
279 culture was incubated at 15 °C for 18 h. The cell pellets were collected and resuspended in 20
280 mL binding buffer (20 mM phosphate buffer (pH 7.4), 500 mM NaCl, 50 mM imidazole, 1 mM
281 dithiothreitol, 1 mM lysozyme, and 1 mM phenylmethylsulfonyl fluoride, and 0.25 mM
282 CuSO₄), followed by ultrasonic decomposition. The target proteins were further purified by
283 Mag-Beads His-Tag Protein Purification Kit (BBI Co Ltd., China) with washing buffer (20 mM
284 phosphate buffer (pH 7.4), 500 mM NaCl, 100 mM imidazole, 0.1% NP-40, 0.25 mM CuSO₄)
285 and elution buffer (20 mM phosphate buffer (pH 7.4), 500 mM NaCl, and 500 mM imidazole).
286 The purified proteins were concentrated by 30K Amicon Ultra-15 (Millipore Co Ltd., USA).
287 The concentration of the purified proteins was measured by Bradford Protein Assay Kit
288 (Beyotime Bio Co Ltd., China) and analyzed by a 12% SDS-PAGE gel (Biomed Co Ltd.,
289 China). The three-dimensional structures of BODs were built by the I-TASSER server (Zhang
290 2008).

291 2.8. *Bilirubin oxidation activity measurement*

292 The BOD activity was measured as previously described (Sakasegawa et al. 2006). Briefly,

293 10 μ L of 40 μ M purified proteins were inoculated into a 300 μ L reaction system containing
294 240 μ L citrate-phosphate buffer (0.1 M, pH 7.5) and 50 μ L bilirubin (2 mM) (Sigma, USA).
295 The oxidation of bilirubin at 40 $^{\circ}$ C by the purified proteins was monitored by a
296 spectrophotometer (Infinite[®] M Plex, Tecan Trading AG) at 450 nm for 3 min. One unit of
297 BOD activity was defined as the amount of BOD (mmol) that oxidized 1 mmol of bilirubin per
298 minute.

299 2.9. Data availability

300 The 16S rRNA gene raw reads were deposited into the NCBI short-reads archive database
301 under the accession number SRR11309782. Raw metagenomic and metatranscriptomic
302 sequences were submitted to NCBI under BioProject PRJNA526440. The MAG of *Ca.*
303 *Loosdrechtia aerotolerans* is available in NCBI GenBank under the accession number
304 SOER00000000.

305 3. Results and Discussion

306 3.1. Identification of a new genus of anammox bacteria

307 Zentraldeponie Emscherbruch (ZDE) WWTP was designed to treat landfill leachate. The
308 plant was designed to remove ammonium through a two-stage process, in which part of
309 ammonium was oxidized to nitrite by the activated sludge system and the remaining
310 ammonium and oxidized nitrite were then transferred to nitrogen gas by anammox in the
311 activated carbon modules under anaerobic condition (Table S1, Figure S1). Biofilm samples
312 were collected from the activated carbon modules of the plant in November 2017 and April
313 2018 for 16S rRNA gene amplicon sequencing and metagenomic and metatranscriptomic
314 sequencing, respectively. In total 27 OTUs of *Brocadiales* anammox bacteria were obtained
315 from 16S RNA gene amplicon sequencing, and most of them were assigned to *Ca.* *Brocadia*,
316 but only OTU27 could not be assigned to any of the known anammox genera (Figure S2).

317 Shotgun metagenomic and metatranscriptomic sequencing of the biofilm produced 251.6
318 million DNA and 66.4 million cDNA reads. In total 198 MAGs were obtained after *de novo*
319 assembly and binning of the metagenomic DNA reads, in which 106 MAGs had high
320 completeness ($> 80\%$) and low contamination ($< 10\%$) (Table S6). Four high-quality anammox
321 bacterial MAGs (Table S7) were identified based on the taxonomic assignments of GTDB-Tk
322 (Chaumeil et al. 2019), including two *Ca.* *Kuenenia* MAGs (YC6 and YC7), one *Ca.* *Brocadia*

323 MAG (YC2), and the MAG YC1. *Ca. Kuenenia* YC6 dominated the anammox community
324 (5.82%), then followed by YC2 (1.85%), YC7 (0.78%), and YC1 (0.6%) (Table S7 and Figure
325 S3). YC1 was assigned to the family *Brocadiaaceae* but could not be assigned to any known
326 genera. In line with this observation, the 16S rRNA gene of YC1 had a 100% identity with
327 OTU27 (Figure S4). In the V4 region of the 16S rRNA gene from YC1 and OTU27, a 7-bps
328 gap was found compared to the 16S rRNA genes from other known anammox bacteria (Figure
329 S4).

330 In line with the finding in “*Ca. Jettenia asiatica*” (Quan et al. 2008), the 16S rRNA,
331 intergenic spacer region, and 23S rRNA coding genes were arranged in a large rRNA gene
332 fragment in YC1. Phylogenetic analyses of the full-length 16S rRNA genes (Figure 1a) and
333 23S rRNA genes (Figure S5c), 43 concatenated markers (Figure S5a), and HzsA sequences of
334 anammox bacteria (Figure S6) confirmed the placement of YC1 in the phylum *Planctomycetes*.
335 Based on the phylogenetic analyses of the 16S rRNA gene (Figure 1a) and HzsA (Figure S6),
336 YC1 had the closest phylogenetic relationship with *Ca. Anammoxoglobus*. The highest 16S
337 rRNA gene sequence identity between YC1 and known anammox bacteria was 92.79% with
338 *Ca. Anammoxoglobus propionicus* (KC862502.1) (Figure 1b), which is much lower than the
339 minimum similarity cutoff demarcating the genus level (94.5%) (Yarza et al. 2014). AAI
340 between YC1 and non-marine genera *Ca. Jettenia*, *Ca. Brocadia*, and *Ca. Kuenenia* was 66.4-
341 75.2% which is larger than the defined minimum genus demarcation using AAI (60-80%)
342 (Konstantinidis et al. 2017, Luo et al. 2014) (Figure S5b). YC1 had the lowest AAI (< 60%)
343 with marine genus *Ca. Scalindua* (Figure S5b). However, AAI among the other three non-
344 marine genera *Ca. Jettenia*, *Ca. Brocadia*, and *Ca. Kuenenia* were also larger than 60% (Figure
345 S5b), illustrating the minimum genus demarcation of AAI for non-marine anammox bacteria
346 should be larger than 60%. Therefore, we propose YC1 represents a new genus and have
347 tentatively named it “*Candidatus Loosdrechtia aerotolerans*”.

348 Description of *Candidatus Loosdrechtia aerotolerans* **gen. nov., sp. nov.** The genus name
349 *Loosdrechtia* (Latin substantive in nominative singular, gender: feminine), is Latinized from
350 van Loosdrecht, in honor of Mark van Loosdrecht for his contribution to the field of anammox
351 research. The specific epithet *aerotolerans* (compounded from L. *aer-*, air, and L. *tolerans*,
352 tolerating, treated as Latin adjective in feminine nominative singular), referring to the oxygen
353 (air) tolerance of the niche of the species.

354 The analogous 16S rRNA gene sequence of “*Ca. Loosdrechtia aerotolerans*” could be
355 detected in 831 rRNA amplicon datasets indexed by IMNGS (Ilias et al. 2016) with a 94.5%

356 identity cutoff (Yarza et al. 2014) and had considerable abundance (> 0.1%) in 379 amplicon
357 datasets. It appeared to be widely distributed in freshwater, sediment, and soil ecosystems as
358 well as in wastewater, activated sludge, and biofilm niches of wastewater treatment systems
359 (Figure S7).

360 3.2. Central anammox catabolism of “*Ca. Loosdrehtia aerotolerans*”

361 The production and oxidation of hydrazine are central for energy conservation in
362 anammox bacteria (Kartal and Keltjens 2016). The biochemically unique multiheme
363 cytochrome *c* protein hydrazine synthase (HZS) produces hydrazine from nitric oxide and
364 ammonium in a slow, two-step reaction mechanism with hydroxylamine as an enzyme-bound
365 intermediate (Dietl et al. 2015, Kartal et al. 2011). HZS and its associated electron transfer
366 module (ETM) are conserved throughout the known anammox genera (Kartal et al. 2011). In
367 line with this observation, HZS and its ETM were encoded by “*Ca. Loosdrehtia aerotolerans*”
368 and were highly conserved (Figure S8a-c, Figure S9). It has been postulated that HZS receives
369 electrons from a tetraheme *c*-type cytochrome, encoded by *kuste2854* in *K. stuttgartiensis* as a
370 part of the ETM (Ferousi et al. 2019). The homolog of this protein in “*Ca. Loosdrehtia*
371 *aerotolerans*” (E3K32_13910) shared a 73% sequence identity with *kuste2854*, and the four
372 heme-binding motifs, including the naturally occurring contracted CKCH heme-binding motif,
373 were all conserved in E3K32_13910 (Figure S10). The amino acid sequences of the three
374 catalytic subunits of HZS (HzsABC) from “*Ca. Loosdrehtia aerotolerans*” were also fully
375 conserved, and superimposable with those in *K. stuttgartiensis* and shared highly similar
376 catalytic sites in the α and γ subunits, including the heme and Zn^{2+} binding sites as well as the
377 specific Hzs β loop in the β subunit (Dietl et al. 2015) (Figure S8a-c, Figure S9). In line with
378 previous findings, the approximately two-fold higher coverage of *hzs* gene than the whole
379 genome (Figure S9) suggests that “*Ca. Loosdrehtia aerotolerans*” also harbors two identical
380 copies of *hzs* gene cluster (Frank et al. 2018, Speth et al. 2015, Yang et al. 2018). As isolated,
381 hydrazine synthase is a relatively slow enzyme, if turnover rate of this enzyme is also slow in
382 the cellular environment, encoding multiple copies might facilitate the increased levels of HZS
383 protein in the cells in order to reach appreciable hydrazine production rates (Kartal et al. 2013).
384 All the three subunits of HZS coding genes were highly transcribed and among the most
385 abundant transcripts (Figure 2, Figure S13), illustrating “*Ca. Loosdrehtia aerotolerans*”
386 participated in nitrogen removal with high activity in the full-scale biofilm system.

387 The oxidation of hydrazine to N_2 results in highly energized, low-potential electrons, which

388 are used to establish a proton motive force for energy conservation and produce reducing
389 equivalents needed for cellular anabolic activity in anammox bacteria. Hydrazine oxidation is
390 carried out by a dedicated octaheme hydroxylamine oxidoreductase-like (HAO-like) protein,
391 hydrazine dehydrogenase (HDH) (Akram et al. 2019, Kartal et al. 2011, Maalcke et al. 2016).
392 The HDH homolog in “*Ca. Loosdrechtia aerotolerans*” (E3K32_09170) was highly conserved,
393 including the catalytic heme and the unusual heme-binding motif (CXXXXCH) (Figure S8d,
394 Figure S11a). HDH is severely inhibited by hydroxylamine which is suggested to leak out of
395 HZS during hydrazine production (Akram et al. 2021, Dietl et al. 2015, Kartal and Keltjens
396 2016, Maalcke et al. 2014). To prevent this inhibition, anammox bacteria encode a dedicated
397 hydroxylamine oxidizing protein (HOX) that recycles hydroxylamine back to NO (Figure 2),
398 which can then be used by HZS (Kartal et al. 2011, Maalcke et al. 2014). In “*Ca. Loosdrechtia*
399 *aerotolerans*”, HOX was also conserved (E3K32_09155) with highly similar heme placements
400 to HOX (kustc1061) of *K. stuttgartiensis* (Figure S8e, Figure S11b). Like HZS, the HDH and
401 HOX coding genes were all highly transcribed and among the most abundant transcripts,
402 indicating the central roles of these enzymes in anammox metabolism (Figure 2, Figure S13).

403 Based on growth experiments with *K. stuttgartiensis* using NO and ammonium, it has been
404 suggested that the core anammox catabolic unit initially consisted of HZS and HDH, and nitrite
405 reduction (NIR) and oxidation (NXR) pathways were acquired later in its evolutionary history
406 (Hu et al. 2019). Indeed, HZS and HDH are conserved throughout the known anammox
407 bacteria, whereas distinct anammox genera utilize different NO-generating nitrite reductases
408 (NIR) (Kartal and Keltjens 2016). *Ca. Kuenenia* and *Ca. Scalindua* species encode cytochrome
409 *cd₁* NIR (NirS), whereas *Ca. Jettenia* species encode a copper-containing NIR (NirK) (Hira et
410 al. 2012, Hu et al. 2012) (Figure 3). “*Ca. Loosdrechtia aerotolerans*” contained a *nirK*, but it
411 was very lowly transcribed (Figure S13). The low transcript of *nir* gene in anammox bacteria
412 has widely been reported (Bagchi et al. 2016, Kartal et al. 2011, Smeulders et al. 2020, Yang
413 et al. 2020c). In striking contrast, NirS is one of the most abundant proteins in “*Ca. Scalindua*
414 *profunda*” (van de Vossen et al. 2013). Although not biochemically characterized, based
415 on physiological experiments as well as transcriptomic and proteomic analyses, the HAO-like
416 protein cluster kustc0458/kustc0457 was implicated in nitrite reduction to NO in *K.*
417 *stuttgartiensis* (Hu et al. 2019). Interestingly, “*Ca. Loosdrechtia aerotolerans*” also encoded
418 and highly transcribed a kustc0458/kustc0457 homolog (Figure S8f, Figure S14), which could
419 fulfill the function of nitrite reduction to NO in this microorganism.

420 The electrons required for nitrite reduction to NO are most likely derived from nitrite

421 oxidation to nitrate catalyzed by NXR (Hu et al. 2019). The highly complex NXR gene cluster
422 identified in *K. stuttgartiensis* (Kartal et al. 2013) was completely conserved in “*Ca.*
423 *Loosdrechtia aerotolerans*” in a single gene cluster (E3K32_04900 to E3K32_04970),
424 including the E3K32_04960, E3K32_04945, and E3K32_04940 encoding NxrA, NxrB, and
425 NxrC, respectively. The transcriptions of these genes were detected, albeit at lower amounts
426 than HZS, HDH, and HOX coding genes (Figure 2, Table S8).

427 3.3. Dissimilatory and assimilatory nitrate reduction

428 DNRA has been observed in the enrichment cultures of anammox bacteria that could
429 supply anammox bacteria with both nitrite and ammonium (Kartal et al. 2007a). In anammox
430 bacteria, the first step of DNRA, nitrate reduction to nitrite, was proposed to be catalyzed by
431 NXR operating in the reverse as nitrate reductase has not been observed in these
432 microorganisms (Chicano et al. 2021, Kartal et al. 2007a). The close affiliation of the “*Ca.*
433 *Loosdrechtia aerotolerans*” NxrA with homologs from the other known terrestrial anammox
434 bacteria was confirmed by phylogenetic analysis (Figure S15), indicating it could be used for
435 nitrate reduction. Pentaheme cytochrome *c* nitrite reductase (NrfA), which catalyzes the six-
436 electron reduction of nitrite into ammonium has been observed in *Ca. Brocadia*, *Ca. Jettenia*,
437 and one *Ca. Scalindua* species (Figure 3). The presence and transcription of NrfA coding genes
438 (Figure 2) are consistent with the possible availability of DNRA can be coupled to the anaerobic
439 oxidation of small organic acids in wastewater treatment systems (Kartal et al. 2007b, Kartal
440 et al. 2008, Lawson et al. 2020, Tao et al. 2019).

441 Interestingly, in contrast to other anammox microorganisms, a soluble, ferredoxin-
442 dependent nitrate reductase (NarB) and its associated ferredoxin related to electron donation
443 (Jepson et al. 2004) were encoded by “*Ca. Loosdrechtia aerotolerans*” (Figure 4a, Figure S12)
444 and had the similar sequencing depth with other genes in the same scaffold (Figure S16a). The
445 nitrate reductase is classified within assimilatory nitrate reductases, had the highest amino acid
446 identity (62.37%) to NarB from the Planctomycete *Aquisphaera giovannonii*
447 (WP_148594665.1) (Figure 4a). NarB is described as a soluble and monomeric enzyme, which
448 contains a [4Fe-4S] cluster and a Mo bismolybdopterin guanine dinucleotide cofactor (Moco)
449 as its prosthetic groups (Rubio et al. 2002). The conserved catalytic sites of the well-studied
450 NarB (CAA52675.1) from *Synechococcus elongatus* (Srivastava et al. 2015, Srivastava et al.
451 2013), including Lys58, Arg70, Cys148, Asp163, and Arg351, were conserved in the “*Ca.*
452 *Loosdrechtia aerotolerans*” NarB (Figure 4b, Figure S16b). The finding of NarB in “*Ca.*

453 *Loosdrehtia aerotolerans*” was unexpected because it has not yet been found in any other
454 anammox bacteria (Figure 3). According to the close lineage between NarB from “*Ca.*
455 *Loosdrehtia aerotolerans*” and other Planctomycete strains (Figure 4a), we propose that the
456 ancestor of anammox bacteria should encode NarB, but it was lost by most of the known
457 anammox bacteria in the long-term evolution might be because of the dramatic changes in the
458 habitat. Nevertheless, the possibility that “*Ca. Loosdrehtia aerotolerans*” acquired the *narB*
459 through horizontal gene transfer from another Planctomycete organism cannot be excluded.

460 Ferredoxin-dependent NarB has been characterized as a crucial enzyme for nitrate
461 assimilatory purposes in diverse microorganisms by catalyzing the two-electron reduction of
462 nitrate to nitrite (Feng et al. 2014, Rubio et al. 1996, Wang et al. 2011). Although the *in situ*
463 transcription of the genes encoding NarB and its associated ferredoxin was not detected (Figure
464 2), “*Ca. Loosdrehtia aerotolerans*” could potentially use this as an additional pathway for
465 nitrate reduction under nitrate replete conditions. As using ferredoxin to produce auxiliary
466 nitrite would be a huge energy waste that nitrate reduction catalyzed by NarB may probably be
467 restricted to ammonium limited conditions for assimilation purposes. But gene coding for
468 known assimilatory nitrite reductase was not found in the recovered part of “*Ca. Loosdrehtia*
469 *aerotolerans*”. Possessing multiple routes for small organic acid utilization coupled with nitrate
470 reduction to ammonium and the ability to use different nitrogen sources could be associated
471 with the niche adaptability of “*Ca. Loosdrehtia aerotolerans*”.

472 3.4. Utilization of organic substrates

473 In anammox bacteria, nitrate reduction to ammonium via nitrite can be coupled to the
474 anaerobic oxidation of small organic acids (Kartal et al. 2007b, Kartal et al. 2008, Lawson et
475 al. 2020, Tao et al. 2019). In agreement with previous findings that at least three different
476 acetyl-CoA synthetases (ACS) were found in anammox bacterial genomes (Kartal et al. 2007b,
477 Kartal et al. 2008), four ACSs were encoded by “*Ca. Loosdrehtia aerotolerans*” and
478 transcription of three of them were detected (Figure 2, Table S8). ACS, which catalyzes the
479 ligation of acetate with CoA for acetyl-CoA production has been implicated in acetate oxidation
480 by anammox bacteria (Russ et al. 2012), but the exact propionate oxidation pathway is still
481 unclear. Nevertheless, substrate specificity studies in different organisms demonstrated that
482 propionate could also be used by ACS with propionate-CoA production (Hele 1954, Li et al.
483 2011, Sealy-Lewis 1994). Additionally, the propionate activation capability of an ACS-like
484 protein (kustc1128) found in *K. stuttgartiensis* was demonstrated in a heterologous host (Russ

485 et al. 2012). The produced propionate-CoA could be further transformed to succinyl-CoA
486 through an α -carboxylation reaction and then to acetyl-CoA through the TCA cycle (Figure 2),
487 which is the pathway for propionate conversion in a syntrophic propionate-oxidizing bacterium
488 (Plugge et al. 1993). All three genes encoding the α -carboxylation pathway were encoded and
489 two of them were transcribed by “*Ca. Loosdrechtia aerotolerans*” (Figure 2, Table S8). The
490 transcribed genes related to acetate and propionate oxidation, suggesting that small organic
491 acid oxidation was active in “*Ca. Loosdrechtia aerotolerans*”. Therefore, we propose that “*Ca.*
492 *Loosdrechtia aerotolerans*” could use the available small organics in wastewater as electron
493 donors for certain redox reactions, such as nitrate/nitrite assimilatory or oxygen elimination
494 (see below). This capability would give “*Ca. Loosdrechtia aerotolerans*” a competitive advantage
495 over other microorganisms in the dynamic wastewater treatment environments, where substrate
496 concentrations might fluctuate. All known anammox bacteria have the genetic potential for
497 acetate conversion, but the homologs of the complete α -carboxylation pathway for propionate
498 transformation were identified only in “*Ca. Loosdrechtia aerotolerans*” and three *Ca. Brocadia*
499 genomes (Figure 3). The capabilities and efficiencies of co-oxidation of ammonium and
500 acetate/propionate likely determine the ecological niches of distinct anammox bacteria.

501 “*Ca. Loosdrechtia aerotolerans*” also encoded the genetic potential to replenish the
502 intracellular carbon cycle using other extracellular organic compounds, such as proteins,
503 peptides, amino acids, long-chain fatty acids, maltodextrin, and C4-dicarboxylate, and to store
504 carbon and energy in the form of glycogen (see the supplemental material: Utilization of other
505 organic substrates and Storage compound).

506 3.5. Diverse oxygen resistance strategies of anammox bacteria

507 Next to the utilization of alternative energy conservation pathways, resistance and
508 adaptability of anammox bacteria to changing environmental conditions plays an important
509 role in the niche differentiation of these microorganisms (Kartal et al. 2013). The reports from
510 distinct anammox enrichment cultures suggest that anammox bacteria are most likely oxygen
511 tolerant rather than strictly anaerobic (Oshiki et al. 2016b). Nevertheless, the underlying
512 mechanism of oxygen tolerance and the activity of a protein used against oxygen toxicity has
513 not been shown in anammox bacteria before.

514 Like in many other microorganisms, superoxide dismutase and catalase related to
515 oxidative stress resistance were encoded and expressed by “*Ca. Loosdrechtia aerotolerans*”
516 (Figure 2) and thus are well prepared for defense against reactive oxygen species (ROS).

517 Interestingly, the catalase coding gene was absent in some *Ca. Brocadia* and *Ca. Jettenia* strains
518 suggesting that these microorganisms employ different oxygen defense systems (Figure 3).
519 An additional bifunctional catalase-peroxidase was uniquely encoded by *Ca. Scalindua* strains
520 (Figure 3), with both catalase (catalyzes high concentration of H₂O₂) and peroxidase (catalyzes
521 low concentration of H₂O₂) activities (Hillar et al. 2000), may confer a selective advantage to
522 *Ca. Scalindua* when facing frequent oxygen intrusions in the oxygen minimum zones of the
523 ocean (Ulloa et al. 2012). The absence of oxygen tolerance systems in “*Ca. Scalindua rubra*”
524 BSI-1 obtained from the anoxic deep sea (Speth et al. 2017) would make sense (Figure 3),
525 which are not necessary for the niche adaptability of anammox bacteria to the anoxic
526 environment and would be additional energy consumption burdens in cell replication and
527 growth under the oligotrophic environment.

528 Unexpectedly, “*Ca. Loosdrechtia aerotolerans*” encoded a CotA-like multicopper oxidase
529 (MCO) with three specific copper-binding sites (Figure 5a, b, Figure S17). A signal peptide
530 identified at the N-terminal of its sequence indicates that the protein will not reside in the
531 cytoplasm. Whether it is transported to the periplasm or the anammoxosome compartment
532 remains to be determined. The CotA-like protein had a high amino acid sequence identity with
533 the oxygen-utilizing laccases and bilirubin oxidases (BOD), and it clustered into the BOD
534 group (Figure 5c, d). A detailed analysis revealed that putative BOD-like proteins were also
535 found in four *Ca. Brocadia* strains, albeit with low sequence identities (< 40%) with the “*Ca.*
536 *Loosdrechtia aerotolerans*” BOD (Figure 5a, d, Figure S17). Consequently, BODs from “*Ca.*
537 *Loosdrechtia aerotolerans*” (E3K32_04160), “*Ca. Brocadia caroliniensis*” (OOP56653.1), and
538 “*Ca. Brocadia sp. AMX2*” (RIK02322.1) were selected for heterologous expression. The
539 BODs expressed in *E. coli* were further purified and displayed one major band in a denaturing
540 SDS polyacrylamide gel (Figure 5e). The activities of the purified BODs were determined
541 towards bilirubin oxidation (Figure 5f). In line with the suggested role of BODs in oxygen
542 resistance, higher oxygen tolerances were previously observed in the two BOD-positive “*Ca.*
543 *Brocadia caroliniensis*” and “*Ca. Brocadia fulgida*” compared to the two BOD-negative “*Ca.*
544 *Brocadia sinica*” and “*Ca. Brocadia anammoxidans*” (Oshiki et al. 2016b). Although the *in situ*
545 transcription of gene encoding BOD was not detected in “*Ca. Loosdrechtia aerotolerans*”
546 (Figure 2), the oxygen-converting BOD could be used as a protective protein involved in low
547 potential electron carriers used by the anammox bacteria for example in the anammoxosome.

548 A survey of oxygen-active proteins revealed the presence of a varying number of genes that
549 could be involved in oxygen defense in anammox bacteria. *Ca. Kuenenia* and *Ca. Scalindua*

550 contain a terminal *cbb3*-type cytochrome *c* oxidase (Figure 3), which is normally involved in
551 aerobic respiration. In line with this finding, the transcriptions of terminal oxidases were
552 detected previously in an anaerobic anammox bioreactor likely associated with protection
553 against oxygen (Lawson et al. 2017, Richardson 2000). The *cbb3*-type cytochrome *c* oxidase
554 has a high affinity for oxygen (Hamada et al. 2014, Pitcher and Watmough 2004), which might
555 function as an oxygen detoxifying enzyme to protect anammox bacteria against oxygen
556 intrusion in dynamic natural (e.g. oxygen minimum zones in the ocean) and engineered
557 environments such as wastewater treatment plants.

558 4. Conclusions and Implications

559 In the present study, we described the discovery of a new anammox bacterium in the full-
560 scale biofilm landfill leachate treating bioreactor. The nearly complete genome of the novel
561 anammox bacterium, tentatively named “*Ca. Loosdrechtia aerotolerans*”, was constructed by
562 metagenomic analysis. All the genes related to anammox core metabolism are conserved in
563 “*Ca. Loosdrechtia aerotolerans*”. As expected, core genes essential for anaerobic ammonia
564 oxidization were among the most highly transcribed genes, reflecting a high nitrogen removal
565 potential of “*Ca. Loosdrechtia aerotolerans*” in the full-scale biofilm system. The low
566 transcribed *nir* gene indicates “*Ca. Loosdrechtia aerotolerans*” might heavily rely on the HAO-
567 like protein to fulfill the function of nitrite reduction to NO as previously observed in *K.*
568 *stuttgartiensis* (Ferousi et al. 2019). Furthermore, its metabolic versatility related to its survival
569 in unfavorable and fluctuating environmental parameters was investigated. Earlier observations
570 and our findings show that anammox bacteria have a versatile lifestyle, are able to utilize
571 different substrates to survive in distinct dynamic environments. Furthermore, these
572 microorganisms are equipped with diverse strategies to protect themselves against changing
573 environmental conditions, such as oxygen fluctuations, in both manmade and natural
574 ecosystems where they remove ammonium from wastewater or contribute to the input of
575 dinitrogen gas into our atmosphere. Overall, the examined full-scale anammox biofilm system
576 provides an interesting case study of anammox-based nitrogen removal. The discovery of this
577 new genus with high transcriptional activity and metabolic versatility advances our
578 understanding of the phylogenetic diversity, ecophysiology, and niche adaptability of anammox
579 bacteria in full-scale wastewater treatment systems. Future research efforts might aim to exploit
580 the enrichment strategy and unique physiological versatility of novel anammox organisms to

581 optimize anammox-based nitrogen removal from sewage using currently existing and new
582 bioreactor designs.

583

584 **Acknowledgments**

585 This study was funded by Natural Science Foundation of China (Grant Nos. 32100086,
586 3210010286, 91851105, 31970105, 31622002, 32000002), Basic and Applied Basic Research
587 Foundation of Guangdong Province (Grant no. 2020A1515111033, 2021A1515011195,
588 2019A1515110089), National Key Technologies Research and Development Program (Project
589 Number: 2020YFA0910300). BK was supported by the ERC starting grant GreenT 640422 and
590 the Max Planck Society. We would like to thank the constructive comments from Prof. Mark
591 van Loosdrecht to improve this manuscript. We acknowledge the support from Zentrum für
592 Wasser- und Umweltforschung (ZWU) in University of Duisburg-Essen. We also appreciate
593 the collaboration with the AGR Group and LAMBDA Gesellschaft für Gastechnik mbH for
594 their technical assistance. We exclusively appreciate the great efforts from Mr. Volker Rekers
595 and Dr. Uwe Walter from LAMBDA Gesellschaft für Gastechnik mbH for sample collection
596 and transport.

597

598 **Competing interests**

599 All other authors have no competing interests.

600

601 **References**

- 602 Akram, M., Dietl, A., Mersdorf, U., Prinz, S., Maalcke, W., Keltjens, J., Ferousi, C., de Almeida,
603 N.M., Reimann, J., Kartal, B., Jetten, M.S.M., Parey, K. and Barends, T.R.M. 2019. A 192-
604 heme electron transfer network in the hydrazine dehydrogenase complex. *Sci. Adv.* 5 (4),
605 eaav4310.
- 606 Akram, M., Dietl, A., Müller, M. and Barends, T.R.M. 2021. Purification of the key enzyme
607 complexes of the anammox pathway from DEMON sludge. *Biopolymers* 112 (6), e23428.
- 608 Ali, M., Shaw, D.R. and Saikaly, P.E. 2020. Application of an enrichment culture of the marine
609 anammox bacterium “*Ca. Scalindua* sp. AMX11” for nitrogen removal under moderate

610 salinity and in the presence of organic carbon. *Water Res.* 170, 115345.

611 Altschul, S.F., Gish, W., Miller, W., Myers, E.W. and Lipman, D.J. 1990. Basic local alignment
612 search tool. *J. Mol. Biol.* 215 (3), 403-410.

613 Azari, M., Le, A.V., Lübken, M. and Denecke, M. 2018. Model-based analysis of microbial
614 consortia and microbial products in an anammox biofilm reactor. *Water Sci. Technol.* 77
615 (7), 1951-1959.

616 Azari, M., Walter, U., Rekers, V., Gu, J.-D. and Denecke, M. 2017. More than a decade of
617 experience of landfill leachate treatment with a full-scale anammox plant combining
618 activated sludge and activated carbon biofilm. *Chemosphere* 174, 117-126.

619 Bagchi, S., Lamendella, R., Strutt, S., Van Loosdrecht, M.C. and Saikaly, P.E. 2016.
620 Metatranscriptomics reveals the molecular mechanism of large granule formation in
621 granular anammox reactor. *Sci. Rep.* 6.

622 Bankevich, A., Nurk, S., Antipov, D., Gurevich, A.A., Dvorkin, M., Kulikov, A.S., Lesin, V.M.,
623 Nikolenko, S.I., Pham, S., Prjibelski, A.D., Pyshkin, A.V., Sirotkin, A.V., Vyahhi, N.,
624 Tesler, G., Alekseyev, M.A. and Pevzner, P.A. 2012. SPAdes: a new genome assembly
625 algorithm and its applications to single-cell sequencing. *J. Comput. Biol.* 19 (5), 455-477.

626 Ben, L. and Steven, L.S. 2012. Fast gapped-read alignment with Bowtie 2. *Nat. Methods* 9 (4),
627 357-359.

628 Caporaso, J.G., Kuczynski, J., Stombaugh, J., Bittinger, K., Bushman, F.D., Costello, E.K.,
629 Fierer, N., Peña, A.G., Goodrich, J.K., Gordon, J.I., Huttley, G.A., Kelley, S.T., Knights,
630 D., Koenig, J.E., Ley, R.E., Lozupone, C.A., McDonald, D., Muegge, B.D., Pirrung, M.,
631 Reeder, J., Sevinsky, J.R., Turnbaugh, P.J., Walters, W.A., Widmann, J., Yatsunenko, T.,
632 Zaneveld, J. and Knight, R. 2010. QIIME allows analysis of high-throughput community
633 sequencing data. *Nat. Methods* 7 (5), 335-336.

634 Chaumeil, P.-A., Mussig, A.J., Hugenholtz, P. and Parks, D.H. 2019. GTDB-Tk: a toolkit to
635 classify genomes with the Genome Taxonomy Database. *Bioinformatics* 36 (6), 1925-
636 1927.

637 Chicano, T.M., Dietrich, L., de Almeida, N.M., Akram, M., Hartmann, E., Leidreiter, F.,
638 Leopoldus, D., Mueller, M., Sánchez, R., Nuijten, G.H.L., Reimann, J., Seifert, K.-A.,
639 Schlichting, I., van Niftrik, L., Jetten, M.S.M., Dietl, A., Kartal, B., Parey, K. and Barends,
640 T.R.M. 2021. Structural and functional characterization of the intracellular filament-
641 forming nitrite oxidoreductase multiprotein complex. *Nat. Microbiol.*

642 Cho, S., Kambey, C. and Nguyen, V.K. 2020. Performance of Anammox Processes for

643 Wastewater Treatment: A Critical Review on Effects of Operational Conditions and
644 Environmental Stresses. *Water* 12 (1), 20.

645 de Almeida, N.M., Neumann, S., Mesman, R.J., Ferousi, C., Keltjens, J.T., Jetten, M.S.M.,
646 Kartal, B. and van Niftrik, L. 2015. Immunogold localization of key metabolic enzymes
647 in the anammoxosome and on the tubule-like structures of *Kuenenia stuttgartiensis*. *J.*
648 *Bacteriol.* 197 (14), 2432-2441.

649 de Almeida, N.M., Wessels, H.J.C.T., de Graaf, R.M., Ferousi, C., Jetten, M.S.M., Keltjens, J.T.
650 and Kartal, B. 2016. Membrane-bound electron transport systems of an anammox
651 bacterium: A complexome analysis. *Biochim. Biophys. Acta* 1857 (10), 1694-1704.

652 Dietl, A., Ferousi, C., Maalcke, W.J., Menzel, A., de Vries, S., Keltjens, J.T., Jetten, M.S.M.,
653 Kartal, B. and Barends, T.R.M. 2015. The inner workings of the hydrazine synthase
654 multiprotein complex. *Nature* 527 (7578), 394-397.

655 Edgar, R.C. 2013. UPARSE: highly accurate OTU sequences from microbial amplicon reads.
656 *Nat. Methods* 10 (10), 996-998.

657 Feng, H., Sun, Y., Zhi, Y., Wei, X., Luo, Y., Mao, L. and Zhou, P. 2014. Identification and
658 characterization of the nitrate assimilation genes in the isolate of *Streptomyces*
659 *griseorubens* JSD-1. *Microb. Cell. Fact.* 13, 174-174.

660 Ferousi, C., Lindhoud, S., Baymann, F., Hester, E.R., Reimann, J. and Kartal, B. 2019.
661 Discovery of a functional, contracted heme-binding motif within a multiheme cytochrome.
662 *J. Biol. Chem.* 294 (45), 16953-16965.

663 Frank, J., Lückner, S., Vossen, R., Jetten, M., Hall, R., Op den Camp, H. and Anvar, S.Y. 2018.
664 Resolving the complete genome of *Kuenenia stuttgartiensis* from a membrane bioreactor
665 enrichment using Single-Molecule Real-Time sequencing. *Sci. Rep.* 8 (1), 4580-4580.

666 Frank, K. and Sippl, M.J. 2008. High-performance signal peptide prediction based on sequence
667 alignment techniques. *Bioinformatics* 24 (19), 2172-2176.

668 Güven, D., Dapena, A., Kartal, B., Schmid, M.C., Maas, B., van de Pas-Schoonen, K., Sozen,
669 S., Mendez, R., Op den Camp, H.J.M., Jetten, M.S.M., Strous, M. and Schmidt, I. 2005.
670 Propionate oxidation by and methanol inhibition of anaerobic ammonium-oxidizing
671 bacteria. *Appl. Environ. Microbiol.* 71 (2), 1066-1071.

672 Hamada, M., Toyofuku, M., Miyano, T. and Nomura, N. 2014. *cbb3*-type cytochrome *c*
673 oxidases, aerobic respiratory enzymes, impact the anaerobic life of *Pseudomonas*
674 *aeruginosa* PAO1. *J. Bacteriol.* 196 (22), 3881-3889.

675 Hele, P. 1954. The acetate activating enzyme of beef heart. *J. Biol. Chem.* 206 (2), 671-676.

676 Hillar, A., Peters, B., Pauls, R., Loboda, A., Zhang, H., Mauk, A.G. and Loewen, P.C. 2000.
677 Modulation of the activities of catalase-peroxidase HPI of *Escherichia coli* by site-directed
678 mutagenesis. *Biochemistry* 39 (19), 5868-5875.

679 Hira, D., Toh, H., Migita, C.T., Okubo, H., Nishiyama, T., Hattori, M., Furukawa, K. and Fujii,
680 T. 2012. Anammox organism KSU□1 expresses a NirK□type copper□containing nitrite
681 reductase instead of a NirS□type with cytochrome cd 1. *FEBS Lett.* 586 (11), 1658-1663.

682 Hu, Z., Speth, D.R., Francoijs, K.-J., Quan, Z.-X. and Jetten, M. 2012. Metagenome analysis
683 of a complex community reveals the metabolic blueprint of anammox bacterium
684 “*Candidatus* Jettenia asiatica”. *Front. Microbio.* 3, 366.

685 Hu, Z., Wessels, H.J.C.T., van Alen, T., Jetten, M.S.M. and Kartal, B. 2019. Nitric oxide-
686 dependent anaerobic ammonium oxidation. *Nat. Commun.* 10 (1), 1244.

687 Huerta-Cepas, J., Forslund, K., Coelho, L.P., Szklarczyk, D., Jensen, L.J., von Mering, C. and
688 Bork, P. 2017. Fast genome-wide functional annotation through orthology assignment by
689 eggNOG-Mapper. *Mol. Biol. Evol.* 34 (8), 2115-2122.

690 Hyatt, D., Chen, G.-L., LoCascio, P.F., Land, M.L., Larimer, F.W. and Hauser, L.J. 2010.
691 Prodigal: prokaryotic gene recognition and translation initiation site identification. *BMC*
692 *Bioinformatics* 11 (1), 119.

693 Ilias, L., Divya, J., Martin, K., Sabahattin, G., Matthias, H., Dirk, H. and Thomas, C. 2016.
694 IMNGS: A comprehensive open resource of processed 16S rRNA microbial profiles for
695 ecology and diversity studies. *Sci. Rep.* 6 (1), 33721.

696 Jepson, B.J.N., Anderson, L.J., Rubio, L.M., Taylor, C.J., Butler, C.S., Flores, E., Herrero, A.,
697 Butt, J.N. and Richardson, D.J. 2004. Tuning a nitrate reductase for function. The first
698 spectropotentiometric characterization of a bacterial assimilatory nitrate reductase reveals
699 novel redox properties. *J. Biol. Chem.* 279 (31), 32212-32218.

700 Kanehisa, M., Sato, Y. and Morishima, K. 2016. BlastKOALA and GhostKOALA: KEGG tools
701 for functional characterization of genome and metagenome sequences. *J. Mol. Biol.* 428
702 (4), 726-731.

703 Kang, D.D., Froula, J., Egan, R. and Wang, Z. 2015. MetaBAT, an efficient tool for accurately
704 reconstructing single genomes from complex microbial communities. *PeerJ* 3, e1165.

705 Kartal, B., de Almeida, N.M., Maalcke, W.J., den Camp, H.J.O., Jetten, M.S. and Keltjens, J.T.
706 2013. How to make a living from anaerobic ammonium oxidation. *FEMS Microbiol. Rev.*
707 37 (3), 428-461.

708 Kartal, B. and Keltjens, J.T. 2016. Anammox Biochemistry: a Tale of Heme c Proteins. *Trends*

709 Biochem. Sci 41 (12), 998-1011.

710 Kartal, B., Kuypers, M., Lavik, G., Schalk, J., Jetten, M. and Strous, M. 2007a. Anammox
711 bacteria disguised as denitrifiers: nitrate reduction to dinitrogen gas via nitrite and
712 ammonium. Environ. Microbiol. 9 (3), 635-642.

713 Kartal, B., Maalcke, W.J., de Almeida, N.M., Cirpus, I., Gloerich, J., Geerts, W., Op den Camp,
714 H.J.M., Harhangi, H.R., Janssen-Megens, E.M., Francoijs, K.-J., Stunnenberg, H.G.,
715 Keltjens, J.T., Jetten, M.S.M. and Strous, M. 2011. Molecular mechanism of anaerobic
716 ammonium oxidation. Nature 479, 127-130.

717 Kartal, B., Rattray, J., van Niftrik, L.A., van de Vossenberg, J., Schmid, M.C., Webb, R.I.,
718 Schouten, S., Fuerst, J.A., Damsté, J.S., Jetten, M.S.M. and Strous, M. 2007b. *Candidatus*
719 "Anammoxoglobus propionicus" a new propionate oxidizing species of anaerobic
720 ammonium oxidizing bacteria. Syst. Appl. Microbiol. 30 (1), 39-49.

721 Kartal, B., van Niftrik, L., Rattray, J., van de Vossenberg, J.L.C.M., Schmid, M.C., Sinninghe
722 Damsté, J., Jetten, M.S.M. and Strous, M. 2008. *Candidatus* 'Brocadia fulgida': an
723 autofluorescent anaerobic ammonium oxidizing bacterium. FEMS Microbiol. Ecol. 63 (1),
724 46-55.

725 Kimura, Y., Isaka, K. and Kazama, F. 2011. Tolerance Level of Dissolved Oxygen to Feed into
726 Anaerobic Ammonium Oxidation (anammox) Reactor. Journal of Water and Environment
727 Technology 9 (2), 169-178.

728 Konstantinidis, K.T., Rosselló-Móra, R. and Amann, R.J.T.I.j. 2017. Uncultivated microbes in
729 need of their own taxonomy. ISME J. 11 (11), 2399-2406.

730 Kopylova, E., Noé, L. and Touzet, H. 2012. SortMeRNA: fast and accurate filtering of
731 ribosomal RNAs in metatranscriptomic data. Bioinformatics 28 (24), 3211-3217.

732 Kuypers, M.M.M., Marchant, H.K. and Kartal, B. 2018. The microbial nitrogen-cycling
733 network. Nat. Rev. Microbiol. 16, 263-276.

734 Kuypers, M.M.M., Sliemers, A.O., Lavik, G., Schmid, M., Jorgensen, B.B., Kuenen, J.G.,
735 Sinninghe Damste, J.S., Strous, M. and Jetten, M.S.M. 2003. Anaerobic ammonium
736 oxidation by anammox bacteria in the Black Sea. Nature 422 (6932), 608-611.

737 Lawson, C.E., Nuijten, G.H.L., de Graaf, R.M., Jacobson, T.B., Pabst, M., Stevenson, D.M.,
738 Jetten, M.S.M., Noguera, D.R., McMahon, K.D., Amador-Noguez, D. and Lückner, S. 2020.
739 Autotrophic and mixotrophic metabolism of an anammox bacterium revealed by in vivo
740 ¹³C and ²H metabolic network mapping. ISME J.

741 Lawson, C.E., Wu, S., Bhattacharjee, A.S., Hamilton, J.J., McMahon, K.D., Goel, R. and

742 Noguera, D.R. 2017. Metabolic network analysis reveals microbial community
743 interactions in anammox granules. *Nat. Commun.* 8, 15416.

744 Letunic, I. and Bork, P. 2019. Interactive Tree Of Life (iTOL) v4: recent updates and new
745 developments. *Nucleic Acids Res.* 47 (W1).

746 Li, H. and Durbin, R.J.b. 2009. Fast and accurate short read alignment with Burrows–Wheeler
747 transform. *Bioinformatics* 25 (14), 1754-1760.

748 Li, R., Gu, J., Chen, P., Zhang, Z., Deng, J. and Zhang, X. 2011. Purification and
749 characterization of the acetyl-CoA synthetase from *Mycobacterium tuberculosis*. *Acta*
750 *Biochim. Biophys. Sin.* 43 (11), 891-899.

751 Luo, C., Rodriguez-r, L.M. and Konstantinidis, K.T. 2014. MyTaxa: an advanced taxonomic
752 classifier for genomic and metagenomic sequences. *Nucleic Acids Res.* 42 (8), e73.

753 Maalcke, W.J., Dietl, A., Marritt, S.J., Butt, J.N., Jetten, M.S.M., Keltjens, J.T., Barends, T.R.M.
754 and Kartal, B. 2014. Structural basis of biological NO generation by octaheme
755 oxidoreductases. *J. Biol. Chem.* 289 (3), 1228-1242.

756 Maalcke, W.J., Reimann, J., de Vries, S., Butt, J.N., Dietl, A., Kip, N., Mersdorf, U., Barends,
757 T.R.M., Jetten, M.S.M., Keltjens, J.T. and Kartal, B. 2016. Characterization of anammox
758 hydrazine dehydrogenase, a key N₂-producing enzyme in the global nitrogen cycle. *J. Biol.*
759 *Chem.* 291 (33), 17077-17092.

760 Mulder, A., van de Graaf, A.A., Robertson, L.A. and Kuenen, J.G. 1995. Anaerobic ammonium
761 oxidation discovered in a denitrifying fluidized bed reactor. *FEMS Microbiol. Ecol.* 16 (3),
762 177-183.

763 Nguyen, L.-T., Schmidt, H.A., von Haeseler, A. and Minh, B.Q. 2015. IQ-TREE: a fast and
764 effective stochastic algorithm for estimating maximum-likelihood phylogenies. *Mol. Biol.*
765 *Evol.* 32 (1), 268-274.

766 Oshiki, M., Ali, M., Shinyako Hata, K., Satoh, H. and Okabe, S. 2016a. Hydroxylamine-
767 dependent anaerobic ammonium oxidation (anammox) by “*Candidatus Brocadia sinica*”.
768 *Environ. Microbiol.* 18 (9), 3133-3143.

769 Oshiki, M., Satoh, H. and Okabe, S. 2016b. Ecology and physiology of anaerobic ammonium
770 oxidizing bacteria. *Environ. Microbiol.* 18 (9), 2784-2796.

771 Overbeek, R., Olson, R., Pusch, G.D., Olsen, G.J., Davis, J.J., Disz, T., Edwards, R.A., Gerdes,
772 S., Parrello, B., Shukla, M., Vonstein, V., Wattam, A.R., Xia, F. and Stevens, R. 2014. The
773 SEED and the Rapid Annotation of microbial genomes using Subsystems Technology
774 (RAST). *Nucleic Acids Res.* 42 (Database issue), D206-D214.

775 Parks, D., Imelfort, M., Skennerton, C., Hugenholtz, P. and Tyson, G. 2015. CheckM: assessing
776 the quality of microbial genomes recovered from isolates, single cells, and metagenomes.
777 Genome Res. 25 (7), 1043-1055.

778 Pitcher, R.S. and Watmough, N.J. 2004. The bacterial cytochrome cbb3 oxidases. Biochim.
779 Biophys. Acta 1655, 388-399.

780 Plugge, C.M., Dijkema, C. and Stams, A.J.M. 1993. Acetyl-CoA cleavage pathway in a
781 syntrophic propionate oxidizing bacterium growing on fumarate in the absence of
782 methanogens. FEMS Microbiol. Lett. 110 (1), 71-76.

783 Quan, Z.X., Rhee, S.K., Zuo, J.E., Yang, Y., Bae, J.W., Park, J.R., Lee, S.T. and Park, Y.H.
784 2008. Diversity of ammonium-oxidizing bacteria in a granular sludge anaerobic
785 ammonium-oxidizing (anammox) reactor. Environ. Microbiol. 10 (11), 3130-3139.

786 Richardson, D.J. 2000. Bacterial respiration: a flexible process for a changing environment.
787 Microbiology 146 (3), 551-571.

788 Robinson, M.D. and Oshlack, A. 2010. A scaling normalization method for differential
789 expression analysis of RNA-seq data. Genome Biol. 11 (3), R25.

790 Rubio, L.M., Flores, E. and Herrero, A. 2002. Purification, cofactor analysis, and site-directed
791 mutagenesis of *Synechococcus* ferredoxin-nitrate reductase. Photosynth. Res. 72 (1), 13-
792 26.

793 Rubio, L.M., Herrero, A. and Flores, E. 1996. A cyanobacterial narB gene encodes a
794 ferredoxin-dependent nitrate reductase. Plant Mol. Biol. 30 (4), 845-850.

795 Russ, L., Harhangi, H.R., Schellekens, J., Verdellen, B., Kartal, B., Op den Camp, H.J.M. and
796 Jetten, M.S.M. 2012. Genome analysis and heterologous expression of acetate-activating
797 enzymes in the anammox bacterium *Kuenenia stuttgartiensis*. Arch. Microbiol. 194 (11),
798 943-948.

799 Sakasegawa, S.-i., Ishikawa, H., Imamura, S., Sakuraba, H., Goda, S. and Ohshima, T. 2006.
800 Bilirubin oxidase activity of *Bacillus subtilis* CotA. Appl. Environ. Microbiol. 72 (1), 972-
801 975.

802 Schmid, M., Twachtman, U., Klein, M., Strous, M., Juretschko, S., Jetten, M., Metzger, J.W.,
803 Schleifer, K.-H. and Wagner, M. 2000. Molecular evidence for genus level diversity of
804 bacteria capable of catalyzing anaerobic ammonium oxidation. Syst. Appl. Microbiol. 23
805 (1), 93-106.

806 Schmid, M., Walsh, K., Webb, R., Rijpstra, W.I., van de Pas-Schoonen, K., Verbruggen, M.J.,
807 Hill, T., Moffett, B., Fuerst, J., Schouten, S., Sinninghe Damsté, J.S., Harris, J., Shaw, P.,

808 Jetten, M. and Strous, M. 2003. Candidatus “*Scalindua brodae*”, sp. nov., Candidatus
809 “*Scalindua wagneri*”, sp. nov., Two New Species of Anaerobic Ammonium Oxidizing
810 Bacteria. *Syst. Appl. Microbiol.* 26 (4), 529-538.

811 Sealy-Lewis, H.M. 1994. A new selection method for isolating mutants defective in acetate
812 utilisation in *Aspergillus nidulans*. *Curr. Genet.* 25 (1), 47-48.

813 Smeulders, M.J., Peeters, S.H., van Alen, T., de Bruijkere, D., Nuijten, G.H.L., op den Camp,
814 H.J.M., Jetten, M.S.M. and van Niftrik, L. 2020. Nutrient Limitation Causes Differential
815 Expression of Transport- and Metabolism Genes in the Compartmentalized Anammox
816 Bacterium *Kuenenia stuttgartiensis*. 11 (1959).

817 Speth, D.R., Lagkouvardos, I., Wang, Y., Qian, P.-Y., Dutilh, B.E. and Jetten, M.S.M. 2017.
818 Draft genome of *Scalindua rubra*, obtained from the interface above the discovery deep
819 brine in the Red Sea, sheds light on potential salt adaptation strategies in anammox bacteria.
820 *Microb. Ecol.* 74 (1), 1-5.

821 Speth, D.R., Russ, L., Kartal, B., Op den Camp, H.J., Dutilh, B.E. and Jetten, M.S. 2015. Draft
822 Genome Sequence of Anammox Bacterium "Candidatus *Scalindua brodae*," Obtained
823 Using Differential Coverage Binning of Sequencing Data from Two Reactor Enrichments.
824 *Genome Announc.* 3 (1), e01415-01414.

825 Srivastava, A.P., Allen, J.P., Vaccaro, B.J., Hirasawa, M., Alkul, S., Johnson, M.K. and Knaff,
826 D.B. 2015. Identification of amino acids at the catalytic site of a ferredoxin-dependent
827 cyanobacterial nitrate reductase. *Biochemistry* 54 (36), 5557-5568.

828 Srivastava, A.P., Hirasawa, M., Bhalla, M., Chung, J.-S., Allen, J.P., Johnson, M.K., Tripathy,
829 J.N., Rubio, L.M., Vaccaro, B., Subramanian, S., Flores, E., Zabet-Moghaddam, M., Stille,
830 K. and Knaff, D.B. 2013. Roles of four conserved basic amino acids in a ferredoxin-
831 dependent cyanobacterial nitrate reductase. *Biochemistry* 52 (25), 4343-4353.

832 Strous, M., Fuerst, J.A., Kramer, E.H.M., Logemann, S., Muyzer, G., van de Pas-Schoonen,
833 K.T., Webb, R., Kuenen, J.G. and Jetten, M.S.M. 1999. Missing lithotroph identified as
834 new planctomycete. *Nature* 400 (6743), 446-449.

835 Tao, Y., Huang, X., Gao, D., Wang, X., Chen, C., Liang, H. and van Loosdrecht, M.C.M. 2019.
836 NanoSIMS reveals unusual enrichment of acetate and propionate by an anammox
837 consortium dominated by *Jettenia asiatica*. *Water Res.* 159, 223-232.

838 Thomas Nordahl, P., Søren, B., Gunnar Von, H. and Henrik, N. 2011. SignalP 4.0:
839 discriminating signal peptides from transmembrane regions. *Nat. Methods* 8 (10), 785–
840 786.

841 Ulloa, O., Canfield, D.E., DeLong, E.F., Letelier, R.M. and Stewart, F.J. 2012. Microbial
842 oceanography of anoxic oxygen minimum zones. Proc. Natl. Acad. Sci. U. S. A. 109 (40),
843 15996-16003.

844 Unthan, M., Klipp, W. and Schmid, G.H. 1996. Nucleotide sequence of the narB gene encoding
845 assimilatory nitrate reductase from the cyanobacterium *Oscillatoria chalybea*. Biochim.
846 Biophys. Acta 1305 (1), 19-24.

847 van de Vossenberg, J., Wobken, D., Maalcke, W.J., Wessels, H.J., Dutilh, B.E., Kartal, B.,
848 Janssen-Megens, E.M., Roeselers, G., Yan, J. and Speth, D. 2013. The metagenome of
849 the marine anammox bacterium '*Candidatus Scalindua profunda*' illustrates the versatility
850 of this globally important nitrogen cycle bacterium. Environ. Microbiol. 15 (5), 1275-1289.

851 Wang, T.-H., Chen, Y.-H., Huang, J.-Y., Liu, K.-C., Ke, S.-C. and Chu, H.-A. 2011. Enzyme
852 kinetics, inhibitors, mutagenesis and electron paramagnetic resonance analysis of dual-
853 affinity nitrate reductase in unicellular N₂-fixing cyanobacterium *Cyanothece* sp. PCC
854 8801. Plant Physiol. Biochem. 49 (11), 1369-1376.

855 Winkler, M.K.H., Yang, J., Kleerebezem, R., Plaza, E., Trela, J., Hultman, B. and van
856 Loosdrecht, M.C.M. 2012. Nitrate reduction by organotrophic anammox bacteria in a
857 nitritation/anammox granular sludge and a moving bed biofilm reactor. Bioresour. Technol.
858 114, 217-223.

859 Yamada, K.D., Tomii, K. and Katoh, K. 2016. Application of the MAFFT sequence alignment
860 program to large data-reexamination of the usefulness of chained guide trees.
861 Bioinformatics 32 (21), 3246-3251.

862 Yang, Y., Daims, H., Liu, Y., Herbold, C., Pjevac, P., Lin, J.-G., Li, M. and Gu, J.-D. 2020a.
863 Activity and metabolic versatility of complete ammonia oxidizers in full-scale wastewater
864 treatment systems. mBio 11 (2), e03175-03119.

865 Yang, Y., Herbold, C.W., Jung, M.-Y., Qin, W., Cai, M., Du, H., Lin, J.-G., Li, X., Li, M. and
866 Gu, J.-D. 2020b. Survival strategies of ammonia-oxidizing archaea (AOA) in a full-scale
867 WWTP treating mixed landfill leachate containing copper ions and operating at low-
868 intensity of aeration. Water Res. 191, 116798.

869 Yang, Y., Li, M., Li, X.-Y. and Gu, J.-D. 2018. Two identical copies of the hydrazine synthase
870 gene clusters found in the genomes of anammox bacteria. Int. Biodeterior. Biodegrad. 132,
871 236-240.

872 Yang, Y., Pan, J., Zhou, Z., Wu, J., Liu, Y., Lin, J.-G., Hong, Y., Li, X., Li, M. and Gu, J.-D.
873 2020c. Complex microbial nitrogen-cycling networks in three distinct anammox-

874 inoculated wastewater treatment systems. *Water Res.* 168, 115-142.

875 Yarza, P., Yilmaz, P., Pruesse, E., Glockner, F.O., Ludwig, W., Schleifer, K.H., Whitman, W.B.,
876 Euzeby, J., Amann, R. and Rossello-Mora, R. 2014. Uniting the classification of cultured
877 and uncultured bacteria and archaea using 16S rRNA gene sequences. *Nat. Rev. Microbiol.*
878 12 (9), 635-645.

879 Yu, N.Y., Wagner, J.R., Laird, M.R., Melli, G., Rey, S., Lo, R., Dao, P., Sahinalp, S.C., Ester,
880 M., Foster, L.J. and Brinkman, F.S.L. 2010. PSORTb 3.0: improved protein subcellular
881 localization prediction with refined localization subcategories and predictive capabilities
882 for all prokaryotes. *Bioinformatics* 26 (13), 1608-1615.

883 Zhang, Y. 2008. I-TASSER server for protein 3D structure prediction. *BMC Bioinformatics* 9,
884 40-40.

885